Proceedings of the 2018 IEEE/ASME International Conference on Advanced Intelligent Mechatronics (AIM), Auckland, New Zealand, July 9-12, 2018

Modeling method for bolted joint interfaces based on transversely isotropic virtual materials *

Yunjian Zha, Jianfu Zhang*, *Member, IEEE*, Dingwen Yu, Pingfa Feng, Zhihang Lin

***Abstract*—To improve the modeling precision of bolted joint interfaces, an improved transversely isotropic virtual materials model is proposed by introducing a calculation method of elastic modulus of composite materials. The joint interface is regarded as a transversely isotropic virtual material that is rigidly linked to two components with a rotation axis parallel to the normal direction of the interface. The elastic and shear moduli of micro-contact asperities are deduced using Hertz contact theory and fractal geometry. Using the calculation method for a composite, the elastic and shear moduli of the entire joint interface were determined, which enabled the parameters of transversely isotropic virtual material to be determined. The theoretical results obtained using this transversely isotropic virtual material model were compared with experimental ones by comparing the mode shapes qualitatively and the natural frequencies quantitatively. The theoretical shapes of the vibration modes were consistent with the experimental ones, and the errors of the natural frequencies were no more than 5%. Compared with the conventional modeling method for bolted joint interfaces, the modeling precision was greatly improved.**

I. Introduction

Prediction of the static and dynamic characteristics of equipment and optimization of the structure of its components has attracted recent research attention. Bolted joints are widely used to connect different components in machine tool assembly, which results in the generation of many joint interfaces. Approximately 90% of the total damping and 60%–80% of the total stiffness in the structure of a machine tool is associated with these joint interfaces [1-6]. Consequently, it is critical to establish an accurate model for bolted joint interfaces [7-8] to analysis and predict the dynamic characteristic of the structure of machine tools.

The dynamic behavior and modeling methods of bolted joint interfaces have been widely studied both theoretically and experimentally for many years. RWTH Aachen WZL [9] investigated the relationships between the normal and tangential stiffness and the pressure applied to joint interfaces in terms of static and dynamic characteristics. Kim et al. [10] reported that the contact element method has higher precision for bolted joints than several finite element methods. Zhang et al. [11] established a fractal model for tangential stiffness based on contact fractal theory. Tian et al. [12] proposed an virtual material method of bolted joint interfaces in machine tools to simplify the modeling process, and Huang et al. [13] performed bolt preload simulations using the virtual material method proposed by Tian [12]. Liao et al. [2] proposed an isotropic virtual gradient material model by dividing the virtual material into several layers to improve the modeling precision.

To establish a model for joint interfaces, both a spring-damping model and virtual material method should be considered. The dynamic model of joint interfaces is usually simplified into a group of spring and damping elements, which is known as a spring-damping model. However, the precision of this method is low, and this approach neglects the coupling relations between each viscoelastic element and the effects of the material, contact surface parameters, and pre-tightening force. Instead, bolted joint interfaces can be considered virtual materials, and properties such as the elastic and shear moduli, Poisson ratio et al. can be determined using a theoretical method; such an approach is known as a virtual material method. Nevertheless, the elastic modulus of a joint interface obtained by integrating the contribution of the elastic modulus for every micro-contact asperity is not convergent. Therefore, the isotropic material model must be converted into an orthotropic material model, which results in a Poisson ratio beyond the available range [−1, 0.5] in finite element analysis software. To address this issue, a transversely isotropic virtual material [14] was adopted in the model proposed in this work because of the different attributes of a joint interface between the *XOY* plane and the normal direction of the contact area.

To establish a more accurate modeling method, an improved transversely isotropic virtual material method is proposed in the current work. First, a general model for the elastic and shear moduli for each micro-contact asperity was established on account of Hertz contact theory and fractal geometry. Second, the elastic and shear moduli of the entire joint interface were determined using the calculation method for a composite, and then, five parameters of the transversely isotropic virtual material were determined. Finally, the first six natural frequencies and mode shapes of the theoretical and experimental results were compared, and the efficiency of the proposed model was verified.

*Research supported by the National Nature Science Foundation of China (Grant No. 51575301).

Pingfa Feng and Jianfu Zhang* are with the State Key Laboratory of Tribology and Beijing Key Lab of Precision/Ultra-precision Manufacturing Equipments and Control, Tsinghua University, Beijing 100084, China (*corresponding author to provide e-mail: zhjf@tsinghua.edu.cn).

All authors are with the Department of Mechanical Engineering, Tsinghua University, Beijing 100084, China.

978-1-5386-1854-7/18/$31.00 ©2018 IEEE

II. MODELING FOR BOLTED JOINTS

A. Normal and shear contact modulus model of a micro-contact

When viewed under a microscope, a rough contact interface can be characterized by its continuity and statistical self-affinity as well as the non-differentiability Weierstrass–Mandelbrot (W–M) fractal function, which can be described by

$$Z(x) = L\left(\frac{G}{L}\right)^{D-1}\sum_{n=0}^{\infty}\frac{\cos\left(2\pi\gamma^{n}\frac{x}{L}\right)}{\gamma^{(2-D)n}} \tag{1}$$

where $Z(x)$ is the surface height, x is the lateral distance, L is the sample length, D is the fractal dimension, and G is the fractal roughness parameter, γ is the dimension parameter of the spectral density ($\gamma > 1$), its typical value is $\gamma = 1.5$.

A rough contact surface is modeled as being composed of many spherical micro-asperities. To simplify the model, the surface can be modeled as an equivalent rough surface in contact with an assumed rigid plane, as illustrated in Fig. 1.

Based on Hertz contact theory, the normal contact load of an elastic micro-asperity is

$$f_e = \frac{4}{3}E^{*}R^{0.5}\delta^{1.5} \tag{1}$$

where $E^{*} = \left[\left(1-\mu_1^2\right)/E_1 + \left(1-\mu_2^2\right)/E_2\right]$; μ_1, μ_2 are the Poisson ratios of the two contact surfaces; and E_1, E_2 are the elastic moduli of the two contact surfaces.

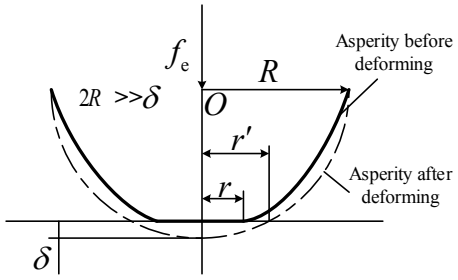

Figure 1. Equivalent model of two micro-asperities

According to the geometric relations, the micro-asperity radius is

$$R \approx \frac{r'^2}{2\delta} = \frac{\pi r'^2}{2\pi\delta} = \frac{a'}{2\pi\delta} = \frac{a'^{0.5D}}{2\pi G^{D-1}} \tag{2}$$

The deformation of the micro-asperity can be described as:

$$\delta = G^{D-1}a'^{1-0.5D} \tag{3}$$

where $a' = \pi r'^2$ is the truncated area of the micro-contact asperity.

Substituting (4) into (2) yields

$$f_e = \frac{4}{3\sqrt{2\pi}}E^{*}G^{D-1}a'^{1.5-0.5D} \tag{5}$$

The normal load for a plastically deformed micro-asperity is

$$f_p = Ha' \tag{6}$$

The deformation of a micro-contact asperity can be divided into two stages, elastic stages and plastic deformation stages, depending on its size, and the deformation is considered to be a continuous process [16]. Therefore,

$$f_p(a_c') = f_e(a_c') \tag{7}$$

The critical truncated area a_c' demarcating the elastic and plastic stages can be determined using (5), (6), and (7) and is expressed as

$$a_c' = \left(\frac{4E^{*}}{3\sqrt{2\pi}H}\right)^{\frac{2}{D-1}}G^{2} \tag{8}$$

Because of the assumption of continuous deformation of micro-contact asperities, the relationship presented in (8) differs from that in [12] and [17].

The statistical size distribution of the truncated area a', which corresponds to the parameter r', as shown in Fig. 1, takes the form

$$n(a') = 0.5D\psi^{1-0.5D}a_L'^{0.5D}a'^{-1-0.5D} \qquad 0<a' \le a_L' \tag{9}$$

where a_L' denotes the truncated area of the largest elastic micro-asperity, and ψ express the domain extension factor for size distribution of the micro-asperity, which satisfies

$$\frac{\psi^{1-0.5D} - \left(1+\psi^{-0.5D}\right)^{-(2-D)/D}}{(2-D)/D} = 1 \tag{10}$$

The normal force F of the entire joint interface can be calculated by integrating the contribution of the elastically and plastically deformed micro-asperities:

$$\begin{aligned} F &= \int_{a_c'}^{a_L'} f_e(a')n(a')da' + \int_{0}^{a_c'} f_p(a')n(a')da' \\ &= \frac{4E^{*}DG^{D-1}}{3\sqrt{2\pi}(3-2D)}\psi^{1-0.5D}a_L'^{0.5D}\left(a_L'^{1.5-D} - a_c'^{1.5-D}\right) \\ &\quad + \frac{DH}{2-D}\psi^{1-0.5D}a_L'^{0.5D}a_c'^{1-0.5D} \end{aligned} \tag{11}$$

The strain and normal stress for an elastic micro-asperity is can be obtained, as show in (12) (13), respectively, according to the definition.

$$\varepsilon = \frac{\delta}{R} \tag{12}$$

$$\sigma = \frac{f_e}{a} \tag{13}$$

where a is the area of an elastic micro-contact, and also can be express as $a = \pi r^2$.

Substituting (5) and (12) into (13) yields

$$\sigma = \frac{4E^*}{3\pi}\sqrt{\varepsilon} \tag{14}$$

Therefore, the elastic modulus of the two micro-contact asperities can be derived:

$$e = d\sigma / d\varepsilon = \frac{2E^*}{3\pi\sqrt{2\pi}} G^{1-D} a'^{0.5D-0.5} \tag{15}$$

According to the report given by Tian et al. [12], the shear modulus between two micro-contact asperities can be described as

$$g_\tau = \frac{16}{\pi}\sqrt[3]{1-\beta/f_\tau}\, G^* \tag{16}$$

Here, β denotes the ratio of the tangential to normal load of the total contact interface; f_τ is the friction coefficient of the contact surfaces; and G^* is the equivalent shear modulus of the two contact surfaces, expressed as $G^* = \left((2\text{-}\mu_1)/G_1 + (2\text{-}\mu_2)/G_2\right)^{-1}$

B. Elastic and shear moduli of contact interface

As show in (17), the elastic modulus of a joint interface obtained by integrating the contribution of the elastic modulus for every micro-contact asperity is normally not convergent.

$$\begin{cases} E = \int_{a_c'}^{a_L'} en(a')da' \\ G_\tau = \int_{a_c'}^{a_L'} g_\tau(a')n(a')da' \end{cases} \tag{17}$$

To solve this problem, a new calculation model of elastic modulus was adopted based on the composite material. As shown in Fig. 2, the general relations between the equivalent elastic modulus and the elastic modulus of each part can be expressed as

$$E = \frac{E_1S_1 + E_2S_2 + E_3S_3}{S_1 + S_2 + S_3} \tag{18}$$

The contact interface of a bolted joint consists of micro-contacts with different elastic moduli. Using the calculation method for a composite material, the elastic and shear moduli of the entire joint interface can be determined. The area of the elastic micro-asperity with truncated area can be described as $n(a')ada'$. Therefore, the normal elastic modulus for the entire joint interface is

$$E = \frac{\int_{a_c'}^{a_L'} en(a')ada'}{A_a} = \frac{E^*DG^{1-D}}{3\pi\sqrt{2\pi}A_a}\psi^{1-0.5D}a_L'^{0.5D}\left(a_L'^{0.5} - a_c'^{0.5}\right) \tag{19}$$

where A_a is the nominal area of the contact region.

Likewise, the shear elastic modulus for the entire joint interface can be expressed as

$$\begin{aligned} G_\tau &= \frac{\int_{a_c'}^{a_L'} g_\tau(a')n(a')ada'}{A_a} \\ &= \sqrt[3]{1-\beta/f_\tau}\,\frac{8DG^*\psi^{1-0.5D}}{(2-D)\pi A_a}a_L'^{0.5D}\left(a_L'^{1-0.5D} - a_c'^{1-0.5D}\right) \end{aligned} \tag{20}$$

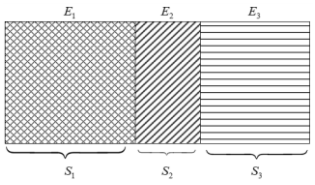

Figure 2. Elastic modulus of composite material

C. Determination of parameters for transversely isotropic virtual materials

A transversely isotropic material is defined by five independent elastic constants, as shown in Fig. 3, namely E_x, E_z, ν_{xy}, ν_{zx} and G_{xz}, and its rotation axis is parallel to the normal direction of the joint interface.

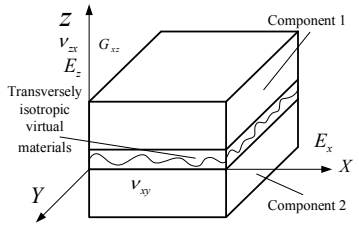

Figure 3. Model of transversely isotropic virtual material

There are many gaps between the surface asperities, whose volume is a small part of entire contact interface. There, in consideration of the contact rate between the two micro-contact asperities, the equivalent elastic modulus of the *X*- or *Y*-axis of the defined virtual material is

$$E_x = \frac{A_r}{A_a}E^* = \frac{\int_0^{a_L'} an(a')da'}{A_a}E^* = \frac{D\psi^{1-0.5D}a_L'}{2(2-D)A_a}E^* \tag{20}$$

where A_r is the real contact area of the contact interface.

In equation (20), the area of an elastic micro-asperity a is used to derive the real contact area of the joint interface instead of the truncated area a' that presented in [14]. Thus, it should contain a_L' as show in (21).

$$E_x = \frac{\int_0^{a_L'} a'n(a')da'}{A_a} E^* = \frac{D\psi^{1-0.5D} a_L}{(2-D)A_a} E^* \tag{21}$$

The parameters of a transversely isotropic material, E_Z and G_{xz} can be assumed to be E and G_τ derived in the previous section of this paper, respectively. There is no need to convert the joint stiffness to the properties of transversely isotropic material.

As for the Passion ration of transversely isotropic material, Zhang et al. [14] suggested that the transverse deformation of a joint interface is closely related to the contact rate of the joint interface. In general, this ratio is so small that the strain of the *X*-axis can be expressed as $\varepsilon_x \approx 0$; thus, the Poisson ratio in the *X–Z* plane can be expressed as $v_{zx} = -\varepsilon_x/\varepsilon_z \approx 0$ .Likewise, $v_{xy} \approx 0$. Thus, the five independent elastic constants of the transversely isotropic material can be expressed as

$$\begin{cases} E_x = \dfrac{D\psi^{1-0.5D} a_L'}{2(2-D)A_a} E^* \\ E_Z = \dfrac{E^* D G^{1-D}}{3\pi\sqrt{2\pi A_a}} \psi^{1-0.5D} a_L'^{0.5D} \left(a_L'^{0.5} - a_c'^{0.5}\right) \\ G_{xz} = \sqrt[3]{1-\beta/f_\tau} \dfrac{8DG^*\psi^{1-0.5D}}{(2-D)\pi A_a} a_L'^{0.5D} \left(a_L'^{1-0.5D} - a_c'^{1-0.5D}\right) \\ v_{xy} = 0, \quad v_{zx} = 0 \end{cases} \tag{22}$$

Combining the new model of elastic and shear moduli of contact interface with the method of transversely virtual material proposed by Zhang [14], the proposed model of this paper was established. The parameters of the transversely isotropic virtual material can be determined using (11) and (22). The area of the virtual material is the same size as the nominal area of the contact region, the thickness of the transversely isotropic virtual material layer is assumed to be 1 mm, and the equivalent density of the virtual material layer can be expressed by the mean density of the two contact surfaces [12].

III. Experimental Verification of Bolted Structure Model

A. Experimental specimens

A block-shaped specimen was designed to validate the proposed model based on transversely isotropic virtual materials, as shown in Fig. 4. The experimental setup consisted of two steel plates (material type Q345 in China) which were connected by four M6 bolts. The thickness of the plates was 20 mm, and the contact area was 150 mm × 60 mm. The pretension of each bolt was controlled to a value of 3 N·m using a torque wrench. The contact surfaces were machined by finish milling to a roughness of Ra3.2.

To determine the parameters for the transversely isotropic virtual material layer, profiles of the contact surfaces were obtained using a Talysurf PGI 1230 roughness tester, and the fractal parameters D=1.569 and G=4.37e−9 m were obtained using the structure function method.

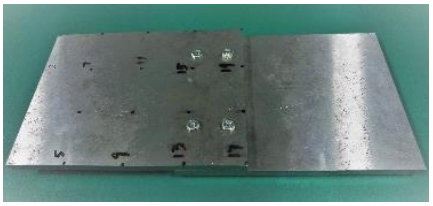

Figure 4. Block-shaped specimen

B. Simulations and experimental results

- Simulation model

3D models of the specimens were obtained using the software Inventor, and the properties of the two steel plates were set to the values listed in TABLE 1. Using the model proposed the parameters of the virtual material were determined by using Matlab to solve (11) and (24), and their value were E_x=4.97e8 Pa, E_z= 4.71e10 Pa, G_{xz}=4.79e8 Pa, υ_{zx}=0, υ_{xy}=0.

TABLE I. THE PROPERTIES OF THE SPECIMEN

Parameter	Elatic modulus（Pa）	Poisson ratio	Density（kg/m3）	Hardness（Pa）
Value	2.05e11	0.3	7850	5.00e8

To verify the efficiency of the proposed method, finite element models for the block-shaped specimen were constructed using the software Workbench and the local coordinate system of the virtual material was set. The virtual material and steel plate were connected in the form of bonded, and the other boundaries were free. A hexahedral mesh was adopted for division, and the virtual material layer was locally refined. The element size of the FEA model, as shown in Fig. 5, was defined 5mm based on the mesh convergence analysis performed.

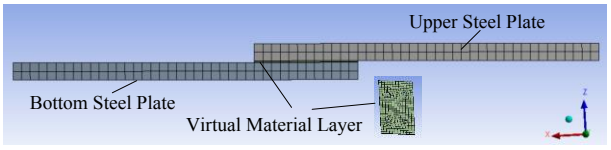

Figure 5. Finite element model of block-shaped specimen

The rotation axis and properties of the transversely isotropic virtual material were defined by using the parameters of orthotropic elasticity. The mode shapes and natural frequencies of the experimental specimen were determined using modal analysis.

- Experimental test

The modal test of the block-shaped specimen was established based on the experimental principle [18] in Fig. 6. The specimen was hung though some elastic ropes to simulate a free boundary. As shown in Fig. 7, acceleration transducers were placed on the test point on the steel plate to record the vibration excited by the PCB impact hammer. The sensitivity of the impact hammer was 12.36 mV/N, and the sensitivity of the acceleration transducer along the *X*-, *Y*-, and *Z*-axis was 102.2, 104, and 101.8 mV/g, respectively. The input of each channel was set as ICP mode.

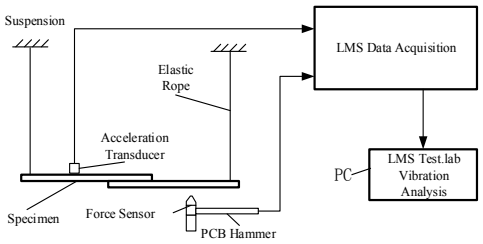

Figure 6. Diagram of modal test of bolted structure

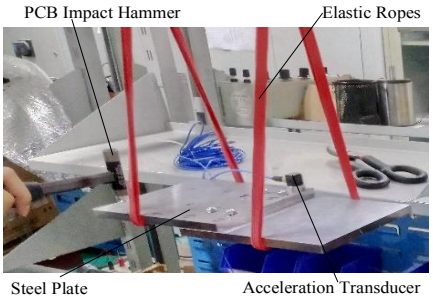

Figure 7. Experimental set-up of bolted structure

The test model of the specimen was established in Lms software, and the vibration of the structure was determined by moving the impact hammer through all the measurement points. In addition, the frequency response of the specimen was recorded, as shown in Fig. 8. The natural frequency and mode shape of the bolted structure were also determined.

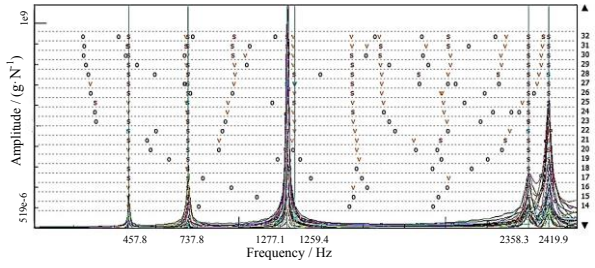

Figure 8. Amplitude frequency response of specimen

- Results and analysis

The comparison results for the first six theoretical and experimental modes of the block-shaped specimen are shown in Fig. 9. The first six theoretical mode shapes were in excellent agreement with the experimental ones.

Furthermore, the conventional virtual material model [17], for which the isotropic virtual material was used by determining the stiffness of the contact region equivalent to the parameters of virtual material, and the bonded method, in which the joint modelled by binding the two contact surfaces, were introduced to verify the accuracy of transversely isotropic virtual materials. The first six orders of natural frequencies of the block-shaped specimen, which were determined by modal experiment and simulated using the transversely isotropic virtual material method, the conventional virtual material model, and bolted method are listed in TABLE 3. For the transversely isotropic virtual material model, the relative errors of the first six orders of the corresponding natural frequencies of the transversely isotropic virtual material model compared with the experimental values were less than 5%. The relative errors of natural frequencies in the first three orders, the most important for engineering applications, were 3%, 0.8%, and −0.6%, respectively. Moreover, compared with the other method, the results of proposed method were much closer to the experimental results and with higher precision in general.

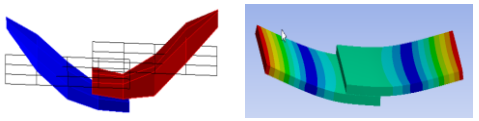

(a) 1st mode shape

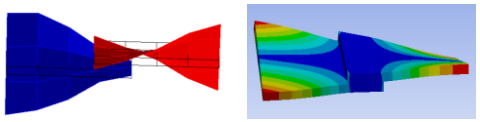

(b) 2nd mode shape

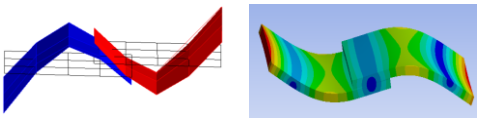

(c) 3rd mode shape

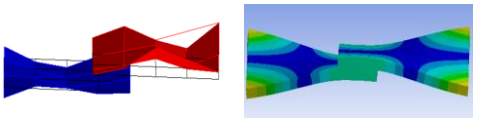

(d) 4th mode shape

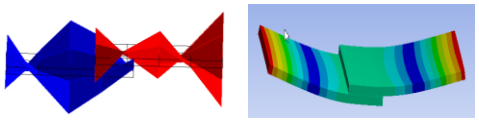

(e) 5th mode shape

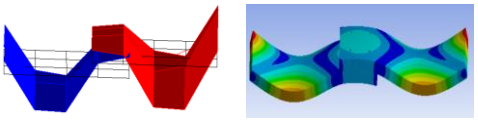

(f) 6th mode shape

Figure 9. Comparison of theoretical (right) and experimental mode shapes(left)

TABLE II. COMPARISON OF NATURAL FREQUENCIES FOR THEORETICAL MODELS WITH EXPERIMENTAL RESULTS.

Natural frequency (Hz)	f_1	f_2	f_3
Experimental results	457.8	737.8	1227.1
Transversely isotropic virtual materials model	472.1	743.7	1219.2
Error of transversely isotropic virtual materials model	3.1%	0.8%	-0.6%
Traditional virtual material method	491.7	834.2	1252.1
Error of traditional virtual material method	7.4%	13.1%	2.0%
Bonded method	516.2	818.7	1243.9
Error of bonded method	12.8%	11.0%	1.3%
Natural frequency (Hz)	f_4	f_5	f_6
Experimental results	1259.4	2358.3	2419.9
Transversely isotropic virtual materials model	1248.5	2417.0	2427.0
Error of transversely isotropic virtual materials model	0.9%	2.5%	0.3%
Traditional virtual material method	1259.1	2477.6	2686.3
Error of traditional virtual material method	0.02%	5.1%	11%
Bonded method	1300.9	2591.2	2695.1
Error of bonded method	3.3%	9.9%	11.4%

IV. CONCLUSION

An improved modeling method for bolted joint interfaces based on transversely isotropic virtual materials was proposed. The normal load of the contact interface and the elastic and shear moduli of a micro-contact were determined using Hertz contact theory and fractal geometry.

Based on the calculation method for composite materials, the elastic and shear moduli of the entire joint interface were obtained, and then the parameters of the transversely isotropic virtual material were obtained.

An impact experiment was designed to verify the efficiency of the proposed method. The theoretical mode shapes were in excellent agreement with the experimental results, and the relative errors of the corresponding natural frequencies in the first three orders for the transversely isotropic virtual material model compared with the experimental values were no more than 5%. In general, the proposed model for bolted joint interfaces was much more precise than the conventional virtual material method.

ACKNOWLEDGMENT

We gratefully acknowledge the financial support for this research from the National Natural Science Foundation of China (Grant No. 51575301).

REFERENCES

[1] B. Fang, L. Zhang, J. Zhao, X. Qu, "Dynamic Parameter Identification and Modeling for Bearing Joint Interface", *J. of Xi'an Jiaotong University*, 46(11), 2012, pp. 69-74.

[2] J. Liao, J. Zhang, P. Feng, D. Yu, Z. Wu, "Interface contact pressure-based virtual gradient material model for the dynamic analysis of the bolted joint in machine tools". *J. of Mechanical Science and Technology*, 30(10), 2016, pp. 4511-4521.

[3] S. T. Wang. "Research on dynamic characteristics and application of typical mechanical interface, M.S. thesis, Kunming University of Science and Technology, 2008.

[4] C. Xu, J. Zhang, P. Feng, D. Yu, Z. Wu, "Characteristics of stiffness and contact stress distribution of a spindle-holder taper joint under clamping and centrifugal forces", *International J. of Machine Tools & Manufacture.* 82-83(7), 2014, pp. 21-28.

[5] C. Xu, J. Zhang, Z. Wu, D. Yu, P. Feng, "Dynamic modeling and parameters identification of a spindle–holder taper joint". *The International J. of Advanced Manufacturing Technology.* 67(5-8), 2013, pp. 1517-1525.

[6] H. Guo, J. Zhang, P. Feng, Z. Wu, D. Yu, "A virtual material-based static modeling and parameter identification method for a BT40 spindle–holder taper joint". *The International J. of Advanced Manufacturing Technology.* 81(1), 2015, pp. 307-314.

[7] C. Xu, J. Zhang, D. Yu, Z. Wu, P. Feng, "Dynamics prediction of spindle system using joint models of spindle tool holder and bearings". *Proc IMechE Part C: J Mechanical Engineering Science.* 229(17), 2015, pp. 3084-3095.

[8] J. Liao, J. Zhang, P. Feng, D. Yu, Z. Wu, "Identification of contact stiffness of shrink-fit tool-holder joint based on fractal theory". *International J. of Advanced Manufacturing Technology*, 90(5-8), 2017, pp. 2173-2184.

[9] Kirsanova VN. "The Shear Compliance of Flat Joints", *J. of Machines and Tooling,* (7), 1967 pp. 23.

[10] J. Kim, J. C. Yoon, and B. S. Kang, "Finite element analysis and modeling of structure with bolted joints", *J. of Applied Mathematical Modelling*, 31(5), 2007, pp. 895-911.

[11] X. L. Zhang et al., "The Elastic-viscoplastic Field of a Steady Propagating Crack Ti", *Chinese J. of Applied Mechanics*, 20(1) (2003) 70-72.

[12] H. L. Tian et al., "Immovable joint surface's model using isotropic virtual material", J. of Vibration Engineering, 26 (4), 2013, pp. 561-573.

[13] K. Huang, J. Jin, "Research on Bolt Preload Simulation Based on Virtual Material Method", *J. of Machinery Design & Manufacture,* (8), 2012, pp. 148-150.

[14] X. Zhang et al., "Modeling Method of Fixed Joint Interface Based on Equivalent Transversely Isotropic Virtual Material", *J. of Mechanical Engineering*, 53(15), 2017, pp. 141-147.

[15] P. Zhong et al., "Finite Element Analysis and Optimization of Medium Truck Frame Based on Hypermesh", *J. of Coal Mine Machinery*, 30(4), 2009, pp. 6-8.

[16] H. Tian, "Normal Revised Model of Joint Interface Distinguishing Elastic and Plastic Deformation", *J. of Mechanical Engineering*, 50(17), 2014, pp. 107-123.

[17] J. Li, "Modeling and application of stiffness characteristics of mechanical fixed interface", M.S. thesis, Huazhong University of Science and Technology, 2011.

[18] J. Liao, D. Yu, J. Zhang, P. Feng, Z. Wu, "An efficient experimental approach to identify tool point FRF by improved receptance coupling technique", International J. of Advanced Manufacturing Technology, (3)2017, pp. 1-10.